Catalysis Today 156 (2010) 306–315

Contents lists available at ScienceDirect

Catalysis Today

journal homepage: www.elsevier.com/locate/cattod

A morphological study of ceramic hollow fibre membranes: A perspective on multifunctional catalytic membrane reactors

Benjamin F.K. Kingsbury, Zhentao Wu, K. Li*

Department of Chemical Engineering, Imperial College London, South Kensington Campus, London SW7 2AZ, UK

ARTICLE INFO

Article history:
Available online 20 March 2010

Keywords:
Asymmetric hollow fibre
Catalyst deposition
Pore size distribution

ABSTRACT

Asymmetric ceramic hollow fibre membranes and membrane supports have been prepared using a combined phase inversion and sintering technique for use in a multifunctional catalytic membrane reactor. The asymmetric structure is such that the fibre may simultaneously function either as a porous membrane and a matrix for catalyst deposition, or as a porous support for the coating of a gas separation layer and a matrix for catalyst deposition. The effectiveness of catalyst deposition depends strongly on the pore size distribution of the membrane or membrane support, which is bimodal in nature and is affected by the calcination temperature and the fibre preparation parameters. The effect of the calcination temperature and preparation parameters on the pore size distribution and fibre morphology have been studied systematically with regard to catalyst deposition and fibre mechanical strength and a route to optimizing the fibre structure has been suggested.

1. Introduction

Membrane reactors combining reaction and separation within the same unit have many advantages over conventional reactor designs. The membrane component of the reactor can either serve to uniformly disperse the reactants prior to their reaction or to selectively separate a product from a reaction mixture. In the latter case, the use of a membrane to separate a product from an equilibrium limited reaction leads to greater conversions and lower operating temperatures [1–3]. By using inorganic hollow fibres with a unique asymmetric pore structure, which have an extremely high surface area to volume ratio and excellent thermal resistance, as either a porous membrane and a matrix for catalyst deposition, or as a porous support for the coating of a gas separation layer and a matrix for catalyst deposition [4], a highly compact multifunctional catalytic membrane reactor can be realized.

An inorganic hollow fibre with an asymmetric pore structure is shown in Fig. 1, and consists of an outer sponge-like region (Region 1), finger-like voids (Region 2), and a region close to the inner fibre surface (Region 3) which may either be occupied by a sponge-like structure or by finger-like voids, depending on the fibre preparation parameters. Unlike previous work [5–7] the combined phase inversion and sintering technique, the details of which are described in detail elsewhere [8], has been employed to generate unique asymmetric structures in a single step. The entrances to the finger-like voids form pores at the inner surface in the absence of an inner sponge-like region, allowing for catalyst to be deposited within the finger-like void structures more easily. In addition, the outer sponge-like region of the fibre may function as either a porous separation layer or as a substrate for the deposition of a separation layer, such as a Pd-based hydrogen permselective membrane [4]. The pore size of the entrances to the finger-like voids present at the fibre surface and the finger-like void volume determine the effectiveness of the catalyst deposition process while the pore size distribution of the sponge-like region is critical in determining the efficiency of the separation process or the quality and thickness of the deposited separation layer. By depositing different catalysts in the finger-like void structures and by depositing an additional separation layer, the developed asymmetric inorganic hollow fibres can thus be used for the construction of a variety of catalytic membrane reactors for a wide range of applications.

In order for the catalytic membrane reactor to function efficiently, the support structure as a whole must produce as little resistance as possible to the permeation of gas. This is achieved by preparing the asymmetric structure mentioned, in which the finger-like voids may be impregnated with catalyst and which minimize resistance to gas permeation, while a palladium membrane may be deposited directly onto the smooth outer surface. The thickness of the sponge-like outer region onto which the palladium membrane is deposited is also minimized and the need to deposit an intermediate layer is eliminated. However, as the sponge-like region provides the bulk of the mechanical strength there is a lower limit to the thickness of this region depending on the application. By varying the spinning suspension composition and the spinning parameters the relative ratios of the finger-like and sponge-like regions, i.e. the thickness of the sponge-like region, can be varied

* Corresponding author. Tel.: +44 207 5945676; fax: +44 207 5945629.
E-mail address: Kang.Li@imperial.ac.uk (K. Li).

0920-5861/$ – see front matter © 2010 Elsevier B.V. All rights reserved.
doi:10.1016/j.cattod.2010.02.039

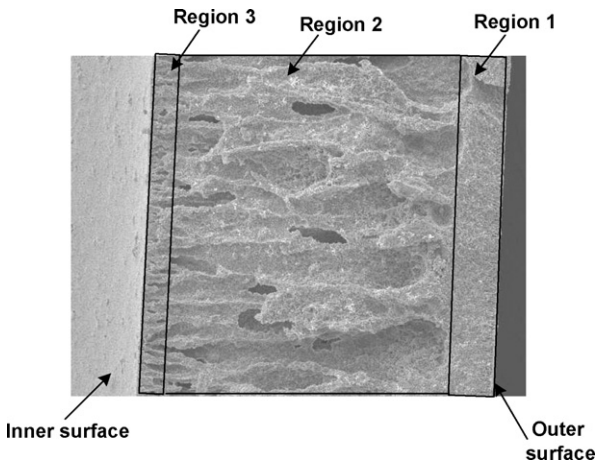

Fig. 1. Cross-sectional SEM image of an asymmetric ceramic hollow fibre consisting of finger-like voids and a sponge-like structure.

systematically [9]. In most cases, the hollow fibre support material cannot function directly as a substrate for catalyst particles so the catalytically active compounds must first be immobilized on a substrate. Deposition of catalyst within the support structure may be achieved in one of three ways. Method 1: Catalyst may be deposited on substrate particles which are then impregnated into the support [4]. Method 2: The catalyst substrate may be deposited in the support, followed by treatment with a homogenous solution containing catalyst precursor compounds [10–13]. Method 3: The support may be treated with a homogenous solution containing both catalyst precursor and catalyst substrate precursor compounds and the catalyst–substrate complex will for "in situ" within the support. However, impregnating a support structure which has a sufficiently small pore size to allow the direct deposition of a palladium layer creates a large, additional, undesired resistance to gas permeation. This problem is exacerbated when depositing catalyst using Method 1 as the catalyst–substrate particles will block pores and may aggregate at the point of entry into the support structure. The same applies to catalyst deposited using Method 2, in which a substrate for the catalyst is deposited prior to the introduction of a solution of catalyst precursors, as both the substrate and catalyst may be deposited in the porous structure of the support. Ideally, the porous separation layer or substrate for a separation layer (sponge-like structure) should not come into contact with catalyst particles, it's pore structure should remain open and unhindered and the catalyst should be contained in the finger-like void structures only. If Region 3 consists of a sponge-like structure, the entrances to the finger-like voids are not present at the inner fibre surface and a degree of "pore blockage" of the inner sponge-like structure is unavoidable. In this case, Method 1 will result in the greatest amount of blockage due to the larger diameter of the catalyst/substrate particles. If the entrances to the finger-like voids are accessible from the fibre surface then "pore blockage" may be eliminated, with a large finger-like void entrance giving rise to more effective catalyst impregnation and lower resistance to gas permeation.

Therefore, the aim of this work is to prepare compact asymmetric inorganic membranes and membrane supports with high surface area to volume ratios, onto which a separation layer can be directly deposited. The support structure must form a suitable matrix for the impregnation of catalyst and must minimize the resistance to gas permeation caused by this process, while at the same time providing sufficient mechanical strength. The effect of increasing the mechanical strength of the support by either increasing the calcination temperature or by increasing the thickness of the sponge-like region has been considered with respect to the ease with which catalyst can be deposited within the support. In addition, factors effecting the formation of pores at both the inner and outer fibre surfaces and the evolution of the pore size distribution as the calcination temperature is increased has been studied in order to optimize the deposition of catalyst within the asymmetric support structure.

It has been shown in this study that asymmetric hollow fibres comprised of finger-like voids and a sponge-like structure exhibit a bimodal pore size distribution and may undergo both coarsening and densification in these regions respectively. It has also been demonstrated that although the pore size distribution of the sponge-like region changes little with variation of parameters during the spinning process, the same cannot be said of the distribution associated with the finger-like voids which may vary greatly, depending on the suspension composition and the spinning parameters. Conversely, while the properties of the sponge-like region change greatly during sintering, the properties of the pores formed by the entrances to the finger-like voids and the finger-like voids themselves resist change.

2. Experimental

2.1. Materials

Aluminium oxide powders 1 μm (alpha, 99.9% metals basis, surface area 6–8 m^2/g), 0.05 μm (gamma–alpha, 99.5% metals basis, surface area 32–40 m^2/g) and 0.01 μm (gamma–alpha, 99.98% metals basis, surface area 100 m^2/g) were purchased from Alfa Aesar (a Johnson Matthey company) and were used as supplied. Polyethersulfone (Radal A300, Ameco Performance, USA), N-methyl-2-pyrrolidone (HPLC grade, Rathbone) and Arlacel P135 (polyethyleneglycol 30-dipolyhydroxystearate, Uniqema) were used as binder, solvent and additive, respectively. Tap water and de-ionized water were used as the external and internal coagulants, respectively.

2.2. Preparation of alumina hollow fibres

A flow diagram showing the stages involved in the preparation of an inorganic hollow fibre is shown in Fig. 2. Arlacel P135 at a concentration of 1.3 wt% was dissolved in NMP/water solutions prior to the addition of aluminum oxide powders (58.7 wt%) at a ratio of

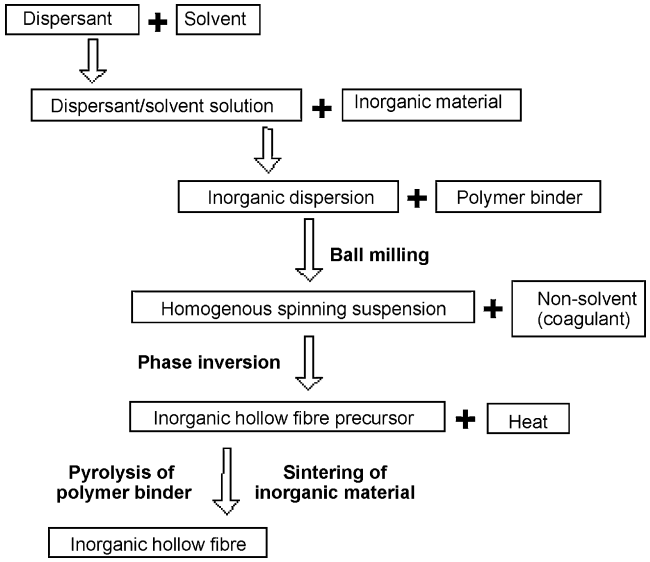

Fig. 2. Flow diagram showing the stages involved in the combined phase inversion and sintering technique for ceramic hollow fibre fabrication.

1:2:7 (0.01 μm:0.05 μm:1 μm). The dispersion was rolled/milled with 20 mm agate milling balls with an approximate alumina/agate weight ratio of 2 for 48 h. Milling was continued for a further 48 h after the addition of PESf (6.1 wt%). The suspension was then transferred to a gas tight reservoir and degassed under vacuum until no bubbles could be seen at the surface.

After degassing, the suspension was transferred to a 200 ml Harvard stainless steel syringe and was extruded through a tube-in-orifice spinneret (ID 1.2 mm, OD 3.0 mm) into a coagulation bath containing 120 l of water (a non-solvent for the polymer) with an air-gap of between 1 and 15 cm. DI water was used as the internal coagulant and the flow rate ranged from 3 to 21 ml/min. The extrusion rate of the spinning suspension and the flow rate of the internal coagulant were accurately controlled and monitored by two individual Harvard PHD 22/2000 Hpsi syringe pumps, ensuring the uniformity of the prepared precursor fibres.

The fibre precursors were left in the external coagulation bath overnight to allow for completion of phase inversion. They were then immersed in an excess of tap water which was replaced periodically over a period of 48 h in order to remove traces of NMP. Finally, the fibre precursors were calcined in air (CARBOLITE furnace) to yield ceramic hollow fibre membranes. The temperature was increased from room temperature to 600 °C at a rate of 2 °C/min and held for 2 h, then to 1000 °C at a rate of 5 °C/min and held for 2 h and finally to the target temperature (1200–1600 °C) at a rate of 5 °C/min and held for 4 h. The temperature was then reduced to room temperature at a rate of 5 °C/min.

2.3. Characterization

Viscosity data was collected (Physica UDS-200 rheometer) at shear rates between 6 and 100 s^{-1} at 20 °C. Spinning suspension samples were taken and tested immediately prior to fibre spinning.

SEM characterization was conducted for sintered fibres which were flexed at ambient temperature until a fracture occurred prior to being mounted on an SEM slide. Samples were gold coated under vacuum for 3 min at 20 mA (EMITECH Model K550) and SEM images at varying magnifications were collected (JEOL JSM-5610 LV).

Mercury intrusion data was collected at absolute pressures of between 1.38×10^3 and 2.28×10^8 Pa (0.2–33,500 psia) (Micromeritics Autopore IV) with an equilibration time of 10 s and assuming a mercury contact angle of 130°. The fibres were broken into sections of approximately 4 mm in length prior to mercury intrusion analysis.

Pore size determination using a gas–liquid displacement technique was undertaken according to an established method [14] using compressed air as the gas and water as the wetting liquid. Fibres of approximately 15 mm in length were fixed into metal holders using epoxy and were sealed at the protruding end also using epoxy. In order to completely wet the hollow fibre, a vacuum was applied to the lumen side while the fibre was immersed in water. The vacuum was maintained for approximately 1 h, during which time water was drawn through the fibre wall into the lumen of the fibre. The fibres were subjected to incrementally increased pressures and the gas flow rate was recorded at each pressure.

3. Results and discussion

After the combination of a desired amount of ceramic powder with a polymer and a solvent, if well mixed, the ceramic/polymer/solvent system can be seen as a suspension of polymer coated ceramic particles. Once immersed in a non-solvent for the polymer (coagulant) which is miscible with the solvent, solvent/non-solvent exchange takes place leading to precipitation of the polymer phase. Ceramic particles are immobilized once precipitation has taken place and the membrane macrostructure can be largely determined at this point by manipulating and adjusting the various parameters of the phase inversion process. As discussed by Kingsbury and Li [9], during the preparation of ceramic hollow fibre membranes using the combined phase inversion and sintering technique, if the suspension viscosity is above a critical value a sponge-like structure is observed. The pore size distribution and porosity of the sponge-like structure after sintering are dependant on properties such as the calcination temperature, the total solids loading, the particle size distribution and the alumina/binder ratio [8,15]. However, below the critical suspension viscosity, viscous fingering takes place resulting in the formation of finger-like voids. If the viscous fingering phenomenon occurs at the nascent fibre surface, the entrances to the finger-like voids will form surface pores which may facilitate catalyst deposition within the finger-like void region of the hollow fibre substrate (Region 2). These pores may vary in size greatly depending on the spinning parameters and will determine the effectiveness of the catalyst deposition process.

3.1. The effect of calcination temperature on the pore size distribution

It can be seen from Fig. 3, showing data for weight and surface area gains after treatment according to Method 1, used by Wu et al. [4] and Method 2, used by Gbenedio et al. [10] that catalyst impregnation into the finger-like void region of the asymmetric ceramic hollow fibre shown in Fig. 4 was achieved using both Methods 1 and 2 discussed above. It can be seen that Method 2, involving the deposition of a mesoporous silica SBA-15 substrate prior to treatment with a solution of catalyst precursors resulted in both a greater weight gain and a larger surface area increase than Method 1, in which γ-alumina particles were treated with a solution of catalyst precursors prior to deposition in the support structure. In addition, in the work by Wu et al. and Gbenedio et al., the efficiency of catalytic membrane reactors prepared using both Method 1 and Method 2, respectively, are compared to fixed bed reactors operating under the same conditions for the dehydrogenation of propane to propene. It has been determined that in both cases, the reactor performance in terms of conversion and selectivity was comparable to that of a FBR due to deactivation of the catalyst as a result of coke formation. However, the volumetric space-time yield and the space-time yield in view of the amount of catalyst used, exceeded the values for the FBR in both catalytic hollow fibre membrane reactor designs. Unfortunately, both Methods 1 and 2 require multiple

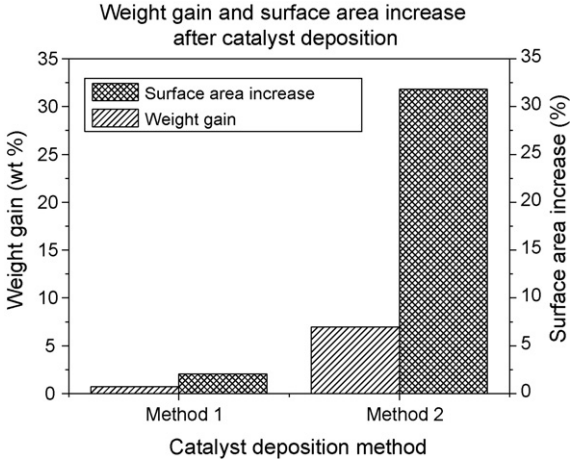

Fig. 3. Weight gain and surface area increase of an asymmetric ceramic hollow fibre after catalyst deposition using two different methods according to Wu et al. and Gbenedio et al.

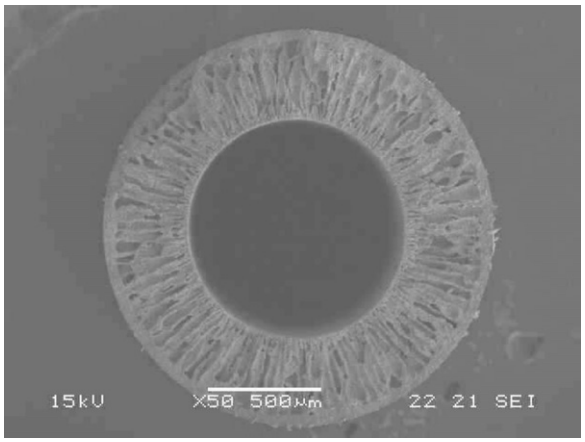

Fig. 4. SEM image of the asymmetric support used by Wu et al. and Gbenedio et al. for catalyst impregnation.

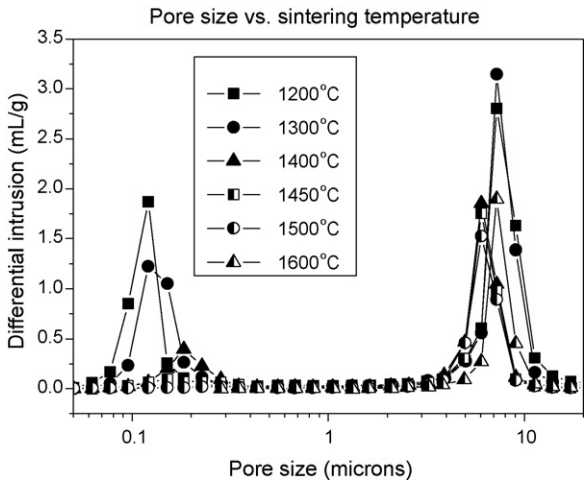

Fig. 5. Mercury intrusion data on pore size vs. calcination temperature for the asymmetric support used by Wu et al. and Gbenedio et al.

steps and are not practical when preparing catalytic membrane reactor modules on a large scale. Therefore, in order to facilitate the impregnation of ready-made catalyst/substrate particles of several microns in size directly into the support structure, it is critical that the entrances to the finger-like voids are present at the fibre surface and are sufficiently large. However, in order to impart the fibre with sufficient mechanical strength for practical applications, a minimum calcination temperature is required, 1450 °C for the fibre used by Wu et al. and Gbenedio et al. shown in Fig. 4, which depends on the fibre morphology. As calcination temperature is a critical factor in determining the mechanical strength of the hollow fibre membrane or membrane support and a minimum calcination temperature is often required, it is important to determine the effect of calcination temperature on the pore size distribution. Therefore, asymmetric hollow fibres were prepared under the same conditions and were calcined at temperatures between 1200 and 1600 °C at intervals of 100 °C with an additional interval at 1450 °C due to the large amount of morphological change that occurs at temperatures between 1400 and 1500 °C. In order to determine the pore size distribution of both through and dead end pores present in the sponge-like region of the fibre, as well as the pores at the inner fibre surface formed by the entrances to the finger-like voids, both mercury intrusion porosimetry and a gas-liquid displacement technique were employed. Mercury intrusion data for fibres calcined at temperatures between 1200 and 1600 °C is shown in Fig. 5. It can be seen from the data that a bimodal pore size distribution exists and that as the calcination temperature is increased from 1200 to 1600 °C the peak pore size of the sponge-like region increases from 0.12 μm at 1200 °C to approximately 0.18 μm at 1400 °C and that this increase is accompanied by a progressive reduction in pore volume which continues up to 1500 °C, after which the sponge-like region is seen to densify [9]. It can be seen from pore size data generated using the gas–liquid displacement technique, Fig. 6, that the peak pore size for the sponge-like region is present between 0.14 and 0.16 μm for fibres prepared under the same conditions and calcined at 1400 and 1450 °C. As only through pores are measured using this technique the pore size distribution of both through and dead end pores present in the sponge-like region of the fibre is shown to compare well, establishing that mercury intrusion porosimetry can be used to infer the pore size of both through and dead end pores. It is not possible, however, to determine the evolution of the pore size distribution during sintering using the gas–liquid displacement technique due to experimental inaccuracies associated with this method and the low mechanical strength of fibres calcined at temperatures below 1400 °C. It can be seen from mercury intrusion data that a reduction in pore size is not observed for the pores at the inner fibre surface formed by the entrances to the finger-like voids, resulting from the viscous fingering phenomenon, represented by the peak between 6 and 7 μm. As the calcination temperature is increased, despite the elimination of porosity and the increase in pore size for the sponge-like region, the pore size of the pores at the inner surface formed by the entrances to the finger-like voids is first reduced slightly to approximately 6 μm and then returns to 7 μm at 1600 °C. Therefore, it has been demonstrated that for fibres prepared under these conditions, finger-like void entrances are open and accessible even at elevated temperature.

3.2. The effect of suspension viscosity on the pore size distribution and fibre morphology

It has been shown that for the fibres used by Wu et al. and Gbenedio et al., the morphology is such that the calcination temperature can be increased to achieve sufficient mechanical strength with no detrimental effect on the size of the entrances to the finger-like voids and hence the effectiveness of catalyst deposition within the support structure. However, due to the unwanted reduction in porosity associated with an increase in calcination temperature it is desirable for this temperature to be reduced. In order for this

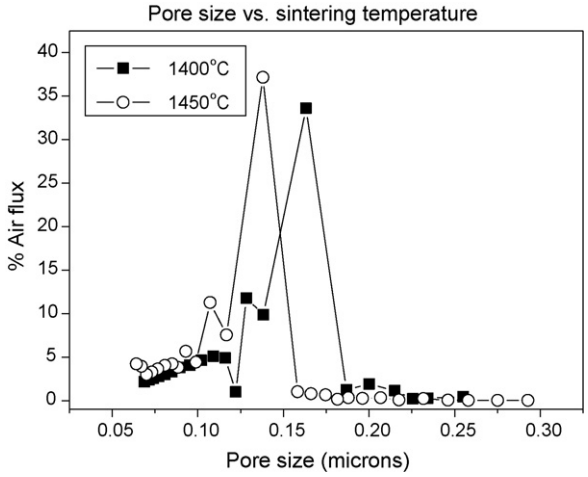

Fig. 6. Gas–liquid displacement data on pore size vs. calcination temperature for the asymmetric support used by Wu et al. and Gbenedio et al. calcined at 1400 and 1450 °C.

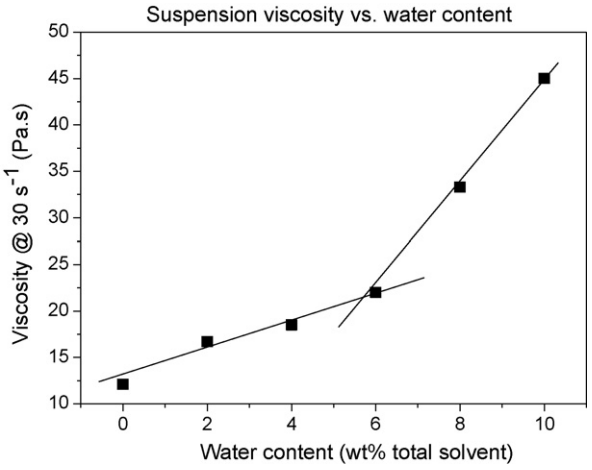

Fig. 7. Viscosity of spinning suspensions prepared with 0–10 wt% water (as a percentage of the total solvent content).

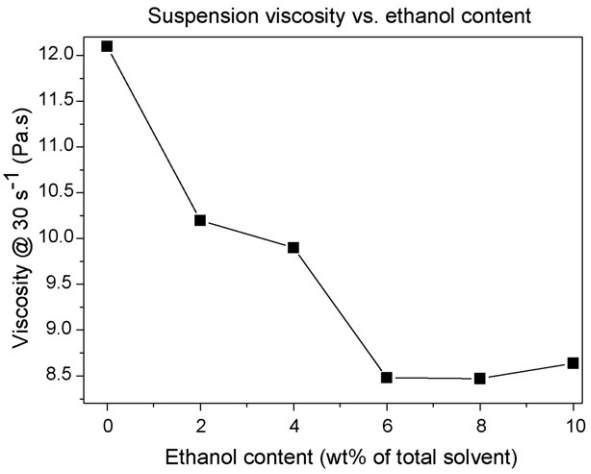

Fig. 9. Viscosity of spinning suspensions prepared with 0–10 wt% ethanol (as a percentage of the total solvent content).

to be done without altering the properties of the spinning suspension, such as the solids loading, particle size distribution and ceramic/polymer ratio and while maintaining sufficient mechanical strength, the relative ratio of the sponge-like region to the finger-like region must be increased.

As discussed by Kingsbury and Li, the relative ratios of the finger-like void and sponge-like regions in asymmetric hollow fibres, i.e. the thickness of the sponge-like region of the fibre can be varied by adding a non-solvent additive to the spinning suspension. This greatly affects not only the initial suspension viscosity but also the rate at which the viscosity increases during the phase inversion process. In order to determine the effect of the suspension viscosity on the pore size distribution, fibres were prepared under the same conditions and at the same calcination temperature used by Wu et al. and Gbenedio et al. but with the addition of 0, 2, 4, 6, 8 and 10 wt% water (as a percentage of the total solvent content) to the spinning suspension. It can be seen from Fig. 7 that the addition of water as a non-solvent additive causes the viscosity to increase to 22.5 Pa s as the concentration of water is increased to 6 wt%. Further addition of water leads to a more dramatic increase up to 45 Pa s at 10 wt% water. The effect of water addition to the spinning suspension is a reduction in the length of finger-like voids and an increase in the thickness of the sponge-like region of the fibre, and is described in detail elsewhere [9]. Inspection of Fig. 8 showing mercury intrusion data for fibres prepared from suspensions containing water as a non-solvent additive clearly shows the dramatic effect that the viscosity increase has on the pore size of the entrances to the finger-like voids. A peak at approximately 0.1–0.2 μm represents the sponge-like region of the fibre and varies little as the concentration of water is increased. This is not the case however for the pores formed by the entrances to the finger-like voids, which are dramatically reduced in size from 5 μm to approximately 1 μm even after the addition of only 2 and 4 wt% water. Further addition of water results in the elimination of this peak indicating that the entrances to the finger-like voids are no longer present at the inner fibre surface. Therefore, despite the presence of finger-like voids and the asymmetry of the hollow fibre cross-section as observed by SEM, the mercury intrusion data shows that addition of water to the spinning suspension first results in a reduction in the size of the pores formed by the entrances to the finger-like voids and then in the formation of a sponge-like region at the inner surface of the fibre (Region 3). In this situation, a peak representing the finger-like voids is not seen in mercury intrusion data. As the finger-like voids are only accessible through a sponge-like region (pore size of approximately 0.12–0.18 μm), in order for mercury to intrude into the finger-like voids, the intrusion pressure must exceed that of the sponge-like region. Consequently, mercury intrusion into the finger-like voids will be included in the intrusion volume of the sponge-like region in the data. Therefore, the presence or absence

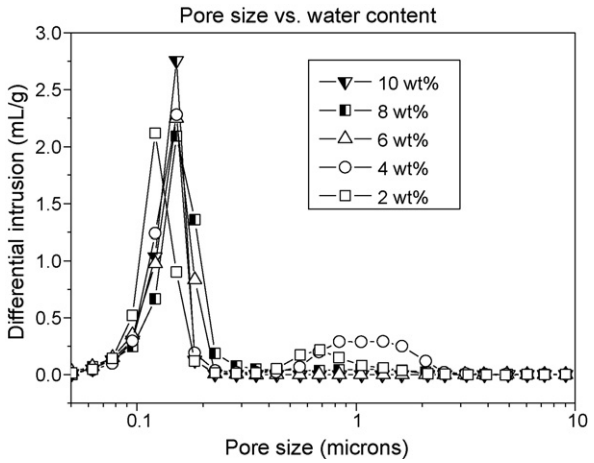

Fig. 8. Mercury intrusion data for fibres prepared with 0–10 wt% water (as a percentage of the total solvent content) calcined at 1200 °C.

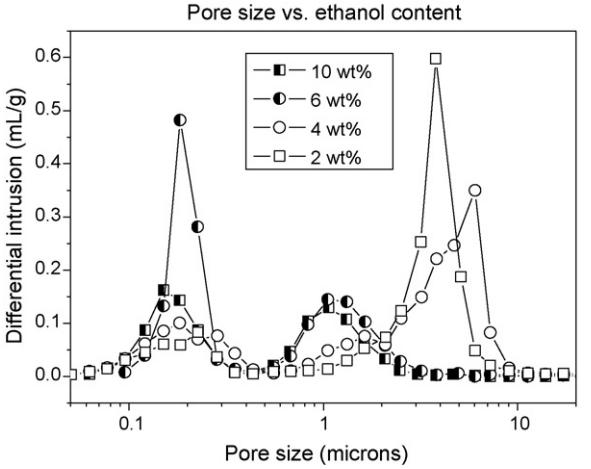

Fig. 10. Mercury intrusion data for fibres prepared with 0–10 wt% ethanol (as a percentage of the total solvent content) calcined at 1450 °C.

of an additional peak in the intrusion data, other than that representing the pores of the sponge-like region, demonstrates whether the finger-like voids are accessible for mercury intrusion and/or catalyst deposition from the fibre surface. If the suspension viscosity is above a critical value, the viscous fingering phenomenon is not observed and finger-like void growth is prevented. In this case, due to the presence of non-solvent in the spinning suspension and the large availability of non-solvent near the surface of the suspension film, the viscosity in this region is prohibitively high and viscous fingering does not occur. However, as non-solvent diffuses further into the suspension film, where the availability of non-solvent is reduced, the concentration of solvent is higher and the suspension viscosity is lower, viscous fingering then occurs and initiates the formation of finger-like voids in this region. Consequently, the morphology that results is that of a sponge-like region at the inner fibre surface and finger-like voids that originate from within the bulk of the fibre. It is not only the initial suspension viscosity that is important in determining the morphology but also the rate of the increase in viscosity once the phase inversion process has been initiated, which is determined by the precipitation

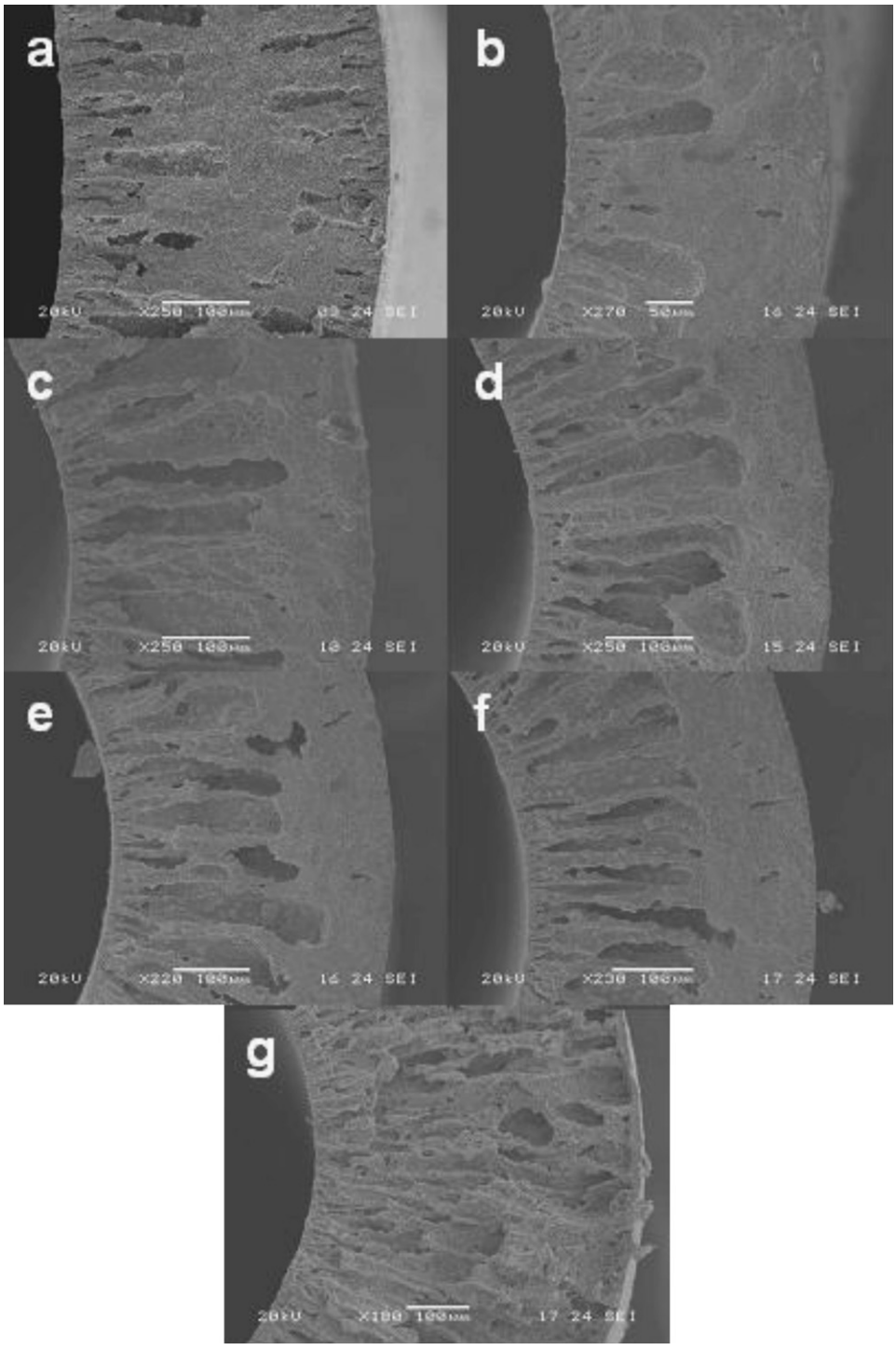

Fig. 11. Cross-sectional SEM images of fibres prepared with varying internal coagulant flow rates and calcined at 1450 °C: (a) 3 ml/min, (b) 6 ml/min, (c) 7 ml/min, (d) 8 ml/min, (e) 9 ml/min, (f) 12 ml/min and (g) 15 ml/min.

rate of the polymer phase. This can be demonstrated by the addition of ethanol as a non-solvent additive to the spinning suspension. Although the solubility of polyethersulfone in ethanol is lower than in NMP but higher than in water, the suspension viscosity initially decreases as the concentration of ethanol is increased and is only seen to increase at higher ethanol concentrations, Fig. 9. The effect of ethanol addition on the pore size of the entrances to the finger-like voids can be seen in Fig. 10. The data shows that the pore size is relatively unchanged at between 4 and 6 μm after the addition of 2 and 4 wt% ethanol to the spinning suspension. In this case it is likely that the reduction in initial suspension viscosity is balanced by the increase in precipitation rate brought about by the addition of ethanol, resulting in little or no change in the pore size. However, as the concentration of ethanol is increased to 6 and 10 wt% the pore size drops to approximately 1 μm despite the reduction in suspension viscosity to 8.5 Pa s, demonstrating the importance of the polymer precipitation rate in determining the pore size of the entrances to the finger-like voids. When controlling the thickness of the sponge-like region by the addition of a non-solvent additive, the pore size of the entrances to the finger-like voids is substantially reduced and finger-like voids may no longer be accessible above a certain non-solvent concentration, depending on the non-solvent in question. Based on this data, it is concluded that increasing the

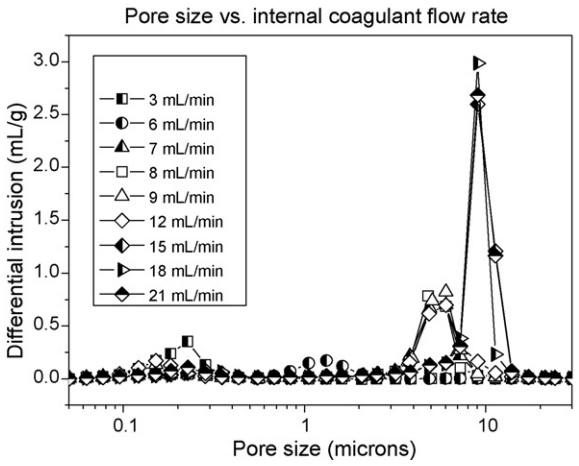

Fig. 12. Mercury intrusion data for fibres prepared with internal coagulant flow rates between 3 and 21 ml/min calcined at 1450 °C.

Fig. 13. Cross-sectional SEM images of fibres prepared with air-gaps between 3 and 13 cm and with an internal coagulant flow rate of 7 ml/min calcined at 1450 °C: (a) 3 cm, (b) 5 cm, (c) 7 cm, (d) 9 cm, (e) 11 cm and (f) 13 cm.

mechanical strength of an asymmetric support by introducing a non-solvent additive into the spinning suspension is an unsuitable method when preparing support structures for catalyst impregnation, due the unfavourable pore size reduction and elimination of the entrances to the finger-like voids present at the inner fibre surface.

3.3. The effect of the internal coagulant flow rate on the pore size distribution and fibre morphology

By varying the internal coagulant flow rate from 3 to 21 ml/min it has been demonstrated that the thickness of the sponge-like region can be varied greatly. SEM images for fibres prepared under the same conditions and at the same calcination temperature used by Wu et al. and Gbenedio et al. but with internal coagulant flow rates of 3, 6, 7, 8, 9, 12 and 15 ml/min are shown in Fig. 11a–g. Mercury intrusion data for fibres prepared with internal coagulant flow rates of 3, 6, 7, 8, 9, 12, 15, 18 and 21 ml/min are shown in Fig. 12. The progressive increase in the thickness of the sponge-like region as the internal coagulant flow rate is decreased is clear from the SEM images and the characteristic bimodal pore size distribution associated with fibres prepared in this way is evident from the mercury intrusion data. In all cases the peak representing the sponge-like region can be found at approximately 0.1–0.2 μm.

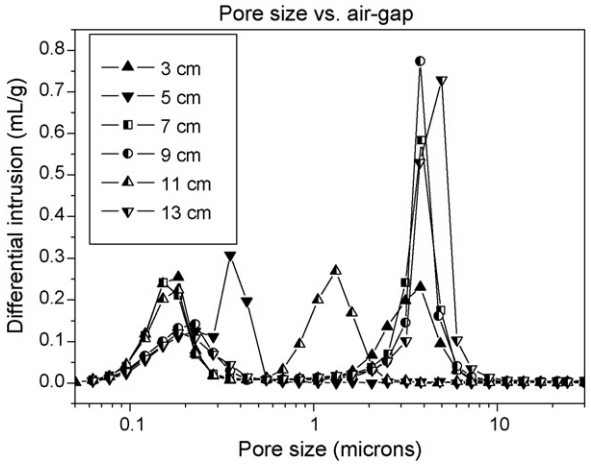

Fig. 14. Mercury intrusion data for fibres prepared with air-gaps between 3 and 13 cm and with an internal coagulant flow rate of 7 ml/min.

However, the peak representing the pores at the inner surface formed by the entrances to the finger-like voids, resulting from the viscous fingering phenomenon, is present at 1.2 μm for a flow rate of 6 ml/min, at approximately 5.5 μm for flow rates of between

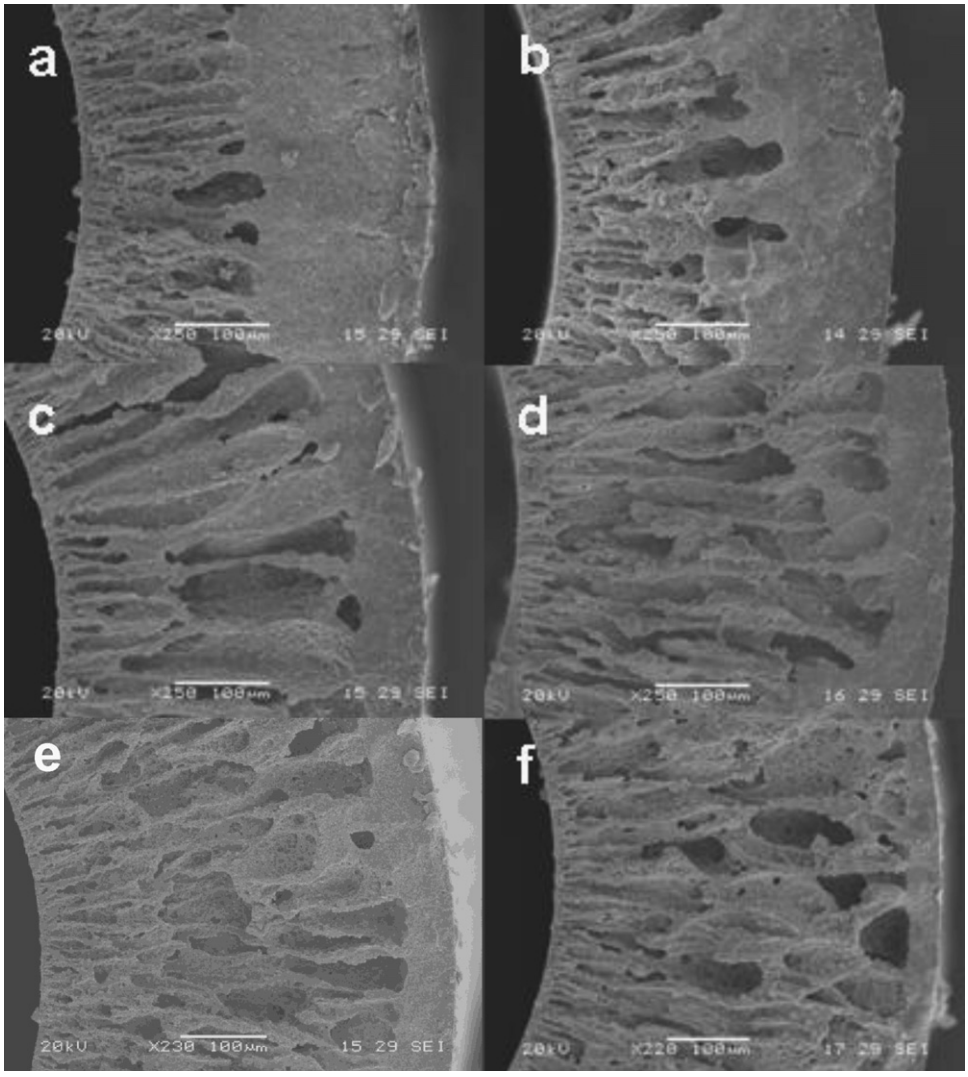

Fig. 15. Cross-sectional SEM images of fibres prepared with air-gaps between 1 and 13 cm and with an internal coagulant flow rate of 12 ml/min calcined at 1450 °C: (a) 1 cm, (b) 3 cm, (c) 7 cm, (d) 9 cm, (e) 11 cm and (f) 13 cm.

7 and 12 ml/min and at 9 μm for flow rates of between 15 and 21 ml/min. Notably absent is a second peak representing the pores formed by the entrances to the finger-like voids for the fibre prepared with an internal coagulant flow rate of only 3 ml/min. In this case, the driving force for the formation of finger-like voids is insufficient to overcome the viscosity of the suspension at the interface between the suspension film and the internal coagulant. Consequently, viscous fingering in not initiated at this interface but is instead initiated within the suspension film itself where the viscosity is lower and a sponge-like region is formed at the inner fibre surface (Region 3), rendering the fibre unsuitable for catalyst impregnation. Also notable in the fibre prepared with an internal coagulant flow rate of 3 ml/min are finger-like voids originating from the shell side of the fibre. A corresponding peak in the mercury intrusion data is also absent, indicating that the finger-like voids do not originate at the outer fibre surface. In this case, finger-like voids are isolated within the sponge-like structure and serve only to reduce the mechanical strength. Based on this data, it is concluded that increasing the mechanical strength of the asymmetric support by reducing the internal coagulant flow rate is an unsuitable method when preparing support structures for catalyst impregnation, due the unfavourable pore size reduction and elimination of the entrances to the finger-like voids present at the inner fibre surface.

3.4. The effect of air-gap on the pore size distribution and fibre morphology

It has been shown by Kingsbury and Li [9] that a variation in the air-gap used during fibre preparation by dry–wet spinning leads to a change in the relative ratios of the finger-like void and sponge-like regions in asymmetric hollow fibres, i.e. a change in the thickness of the sponge-like region of the fibre. It can be seen from the SEM images shown in Fig. 13a–f, of fibres prepared under the same conditions and calcined at the same temperature used by Wu et al. and Gbenedio et al. (1450 °C) but with air-gaps of between 3 and 13 cm and an internal coagulant flow rate of 7 ml/min that a reduction in air-gap gives rise to an increase in the thickness of the sponge-like region and consequently an increase in mechanical strength. However, the appearance of isolated voids in the sponge-like structure, the formation mechanism of which is detailed elsewhere [9], is observed which will lead to a reduction in mechanical strength. In addition, a reduction in the size of the entrances to the finger-like voids is observed from mercury intrusion data, Fig. 14. Due to the relatively low internal coagulant flow rate, finger-like void entrance size is seen to vary greatly with the highest values of between 4 and 5 μm for fibres prepared with air-gaps of 3, 7, 9 and 13 cm and 0.4 and 1.3 μm for fibres prepared with air-gaps of 5 and 11 cm respectively. Both isolated voids and a reduction in the size or elimination of the entrances to the finger-like voids are detrimental to the effectiveness of catalyst impregnation into the asymmetric membrane or membrane support.

Therefore, in an attempt to increase the thickness of the sponge-like region while at the same time retaining an acceptable pore size of the entrances to the finger-like voids, as well as preventing the formation of isolated voids in the sponge-like region, fibres were prepared with air-gaps between 1 and 13 cm and with an internal coagulant flow rate of 12 ml/min. From SEM images, Fig. 15a–f, it is shown that despite the progressive increase in the thickness of the sponge-like region as the air-gap is reduced, accounting for over 50% of the thickness of the fibre cross-section in fibres prepared using an air-gap of only 1 cm, the almost total absence of isolated voids is apparent. In addition, despite the reduction of the length of the air-gap, the mercury intrusion data shown in Fig. 16 demonstrates that the pore size of the entrances to the finger-like voids remains at between 7 and 9 μm. Therefore, the thickness of the sponge-like region and hence the mechanical strength of the fibre can be controlled by varying the air-gap only if the internal coagulant flow rate is sufficient to prevent the formation of isolated voids and to generate an acceptable pore size of the entrances to the finger-like voids.

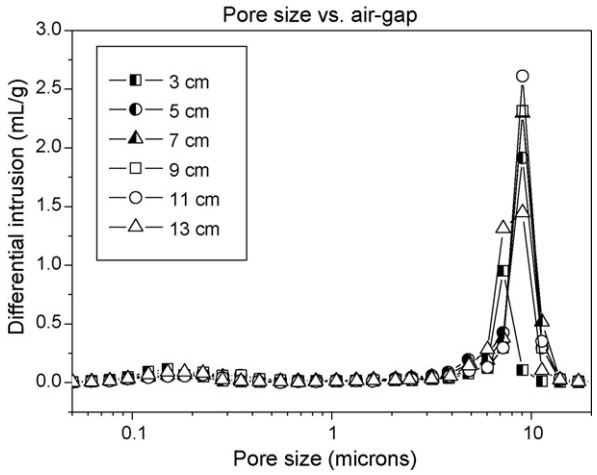

Fig. 16. Mercury intrusion data for fibres prepared with air-gaps between 1 and 13 cm and with an internal coagulant flow rate of 12 ml/min calcined at 1450 °C.

4. Conclusions

Using a combined phase inversion and sintering technique, asymmetric ceramic hollow fibre membranes and membrane supports can be prepared in a single step. Fibres prepared in this way may consist of both finger-like voids and a sponge-like structure in varying ratios. The asymmetric fibre may function as either a porous membrane and a matrix for catalyst deposition, or as a porous support for the coating of a gas separation layer and a matrix for catalyst deposition and may function as a highly compact multifunctional catalytic membrane reactor. Both the pore size distribution of the pores formed by the entrances to the finger-like voids and of the sponge-like region are critical in determining the effectiveness of catalyst deposition and the quality of the separation layer, respectively. It has been shown that an increase in calcination temperature leads to an increase in the mechanical strength of the fibre but this is accompanied by an unwanted increase in the mean pore size of the sponge-like region as well as a decrease in porosity. However, it has also been demonstrated that entrances to finger-like voids that are present at the fibre surface remain open during the calcination process and resist densification, a crucial property that allows for catalyst deposition within the finger-like voids. The mechanical strength of the fibre can also be augmented by increasing the thickness of the sponge-like region, which provides the bulk of the mechanical strength. In order to control the morphology and mechanical strength of the fibre while at the same time maintaining the desired pore structure, a selection of preparation parameters have been varied systematically. It has been shown in this work that by using a non-solvent additive in the spinning suspension and by varying spinning parameters such as the internal coagulant flow rate and air-gap, the viscosity of the suspension during the spinning process and the fibre morphology can be manipulated. The addition of a non-solvent additive to the spinning suspension leads to both an increase in suspension viscosity and an increase in the polymer precipitation rate, resulting in an increase in the thickness of the sponge-like region of the fibre cross-section. The same morphological change results from a reduction in air-gap or internal coagulant flow rate. However, in all three cases, the pore size of the entrances to the finger-like voids is dramatically reduced or even eliminated

altogether and the appearance of isolated voids within the sponge-like structure of the fibre is observed, which cause an undesired reduction in mechanical strength. It has been demonstrated in this work that, in the absence of a non-solvent additive in the spinning suspension and with a sufficiently high internal coagulant flow rate, a reduction in air-gap leads to an increase in the thickness of the sponge-like layer while at the same time maintaining the pore size of the entrances to the finger-like voids, allowing for efficient deposition of catalyst within the hollow fibre support structure. Therefore, by varying these parameters in combination, it is possible to optimize the hollow fibre support structure with respect to the morphology, mechanical strength and pore size distribution.

Acknowledgements

The authors gratefully acknowledge the research funding provided by EPSRC in the United Kingdom (grant no. EP/E000231/1). A project studentship provided by EPSRC to one of the authors, Benjamin F.K. Kingsbury is also gratefully acknowledged.

References

[1] J. Galuszka, R.N. Pandey, S. Ahmed, Catal. Today 46 (1998) 83.
[2] J.N. Armor, J. Membr. Sci. 147 (1998) 217.
[3] H. Weyten, J. Luyten, K. Keizer, L. Willems, R. Leysen, Catal. Today 56 (2000) 3.
[4] Z. Wu, M.D. Irfan Hatim, B.F.K. Kingsbury, E. Gbenedio, K. Li, AIChE J. 55 (2009) 2389.
[5] X.L. Pan, N. Stroh, H. Brunner, G.X. Xiong, S.S. Sheng, Sep. Purif. Technol. 32 (2003) 265.
[6] N.D.A.G.N. Stroh, Proceedings of the 7th ICIM Oral Presentation, 2002.
[7] N.D.U.H.N.S.C. Chaumette, Proceedings of ICOM by the European Membrane Society Poster Presentation, 2002.
[8] S. Liu, K. Li, R. Hughes, Ceram. Int. 29 (2003) 875.
[9] B.F.K. Kingsbury, K. Li, J. Membr. Sci. 328 (2009) 134.
[10] E. Gbenedio, Z. Wu, M.D.I. Hatim, B.F.K. Kingsbury, K. Li. Catal. Today, second review.
[11] T. Valdés-Solís, G. Marbán, A.B. Fuertes, Appl. Catal., B 46 (2003) 261.
[12] E. Crezee, P.J. Kooyman, J. Kiersch, W.G. Sloof, G. Mul, F. Kapteijn, J.A. Moulijn, Catal. Lett. 90 (2003) 181.
[13] T. Valdés-Solís, G. Marbán, A.B. Fuertes, Catal. Today 69 (2001) 259.
[14] P. Mikulasek, P. Dolecek, Sep. Sci. Technol. 29 (1994) 1183.
[15] X. Tan, S. Liu, K. Li, J. Membr. Sci. 188 (2001) 87.